JOURNAL OF SPACECRAFT AND ROCKETS
Vol. 40, No. 5, September–October 2003
This paper reprinted from AIAA Journal, Vol. 5, No. 9, 1967, pp. 1557–1562

Three-Dimensional Flow around Blunt Bodies

GINO MORETTI* AND GARY BLEICH†
General Applied Science Laboratories Inc., A Subsidiary of The Marquardt Corporation, Westbury, N. Y.

The three-dimensional flowfield around blunted bodies traveling at supersonic speed is computed using a time-dependent technique. A similar technique has been used by one of the present authors to compute two-dimensional and axisymmetric flowfields around blunted bodies and has proved to be highly successful when compared with experimental results. The problem is mathematically well posed, the technique is stable, and its accuracy increases with the fineness of the mesh. Values at points within the shock layer are computed with a method closely related to the Lax-Wendroff technique. The shock wave, however, is considered as a moving discontinuity. Values at shock points and at body points are computed by a four-dimensional method of characteristics. In this way, the shock points are defined precisely, and the application of boundary conditions on bodies of any shape becomes easy. In addition, a drastic reduction in computational time is achieved. A three-dimensional flow around a blunt body can be evaluated in 40 min on an IBM 7094 computer. Full detailed examples of computed flowfields are shown.

I. Introduction

FEW reports[1,2,5] have been published thus far on the three-dimensional flow around a blunt body, not for lack of interest, but rather because of some intrinsic difficulties of the problem. Such difficulties are of the same nature as in the two-dimensional or axisymmetrical problem, only they are enhanced by the presence of a third space variable.

In Ref. 3 and, in a more extended form, in Ref. 4, the blunt-body problem depending on two space variables has been analyzed, and reasons for adopting a time-dependent technique of solution were given. In Ref. 2, a time-dependent technique for the three-dimensional problem was presented. However, it is encumbered by a very large number of points to be computed (24,000 in the example) and, consequently, it requires a computational time which is too long to be practical (we estimate about 40 hr on an IBM 7094 for the example given in Ref. 2).

The time-dependent technique of the present paper is the three-dimensional counterpart of the one described in Refs. 3

(Continued on next page)

Presented as Paper 67-222 at the AIAA Fifth Aerospace Sciences Meeting, New York, January 23–26, 1967; submitted January 18, 1967; revision received March 30, 1967. This work was sponsored by the U. S. Atomic Energy Commission through Sandia Corp., Albuquerque, N. Mex. [3.04]

* Scientific Supervisor; now Professor, Polytechnic Institute of Brooklyn, Farmingdale, N. Y. Associate Fellow AIAA.

† Consultant. Associate Member AIAA.

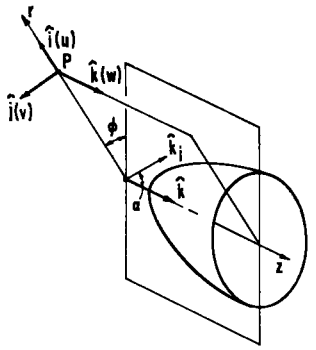

Fig. 1 Frame of reference.

and 4. Its main advantages with respect to the one of Ref. 2 are:

1) The body shape may be assigned arbitrarily.

2) The shock wave is defined as a sharp discontinuity.

3) A reduction of 40 to 1 in the number of mesh points is achieved.

4) Consequently, the computational time is reduced by a factor larger than 50. Because of the small storage required, no additional tapes are needed for temporary storage. Thus, the computational time is further reduced.

Some arguments to support these statements can be found at the end of the paper.

II. General Outline

The gas is assumed to be inviscid and perfect, with a constant ratio of specific heats γ. The body is assumed to be axisymmetric. The flow is assumed to be uniform and supersonic at infinity, and there are three-dimensional effects because the angle α between the velocity at infinity and the body axis is different from zero. All these assumptions, except the first, can be relaxed without changing the logic of the technique. They have been used here only for the sake of simplicity.

A cylindrical frame of reference (r, φ, z) is used where z is the axis of symmetry of the body. The unit vectors are defined in Fig. 1. The velocity components in the **i**, **j**, **k** direction are u, v, and w, respectively.

The $\varphi = 0$ half-plane is defined by the vector **k** and the velocity at infinity ($\mathbf{V}_\infty = q_\infty \mathbf{k}_1$); α is the angle of attack, $\cos\alpha = \mathbf{k}\cdot\mathbf{k}_1$. The body geometry, independent of φ, is defined by the equation

$$z - b(r) = 0 \tag{1}$$

The shock wave is described by a surface

$$z - s(r, \varphi, t) = 0 \tag{2}$$

which is to be computed at each time step. Let p_∞, ρ_∞ be the pressure and density in the freestream, r_{ref} a characteristic length of the body; $t_{ref} = r_{ref}/(p_\infty/\rho_\infty)^{1/2}$. The equations of motion are written in nondimensional form as follows:

$$R_t + uR_r + vR_\varphi/r + wR_z + u_r + v_\varphi/r + w_z + u/r = 0 \tag{3}$$

$$u_t + uu_r + vu_\varphi/r + wu_z + (p/\rho)P_r - v^2/r = 0 \tag{4}$$

$$v_t + uv_r + vv_\varphi/r + wv_z + (p/\rho)P_\varphi/r + uv/r = 0 \tag{5}$$

$$w_t + uw_r + vw_\varphi/r + ww_z + (p/\rho)P_z = 0 \tag{6}$$

$$S_t + uS_r + vS_\varphi/r + wS_z = 0 \tag{7}$$

where pressure and density have been scaled to p_∞ and ρ_∞, velocities to $(p_\infty/\rho_\infty)^{1/2}$, lengths to r_{ref}, and times to t_{ref}. In addition, $P = \ln p$, $R = \ln\rho$, $S = P - \gamma R$.

The problem is solved in a three-dimensional region bounded by the body surface; the bow shock; and a circular cylinder, $r = r_1$. A finite-difference counterpart of Eqs. (3–7) is used for interior points. A special treatment is given to shock and body points.

III. Interior Points

At each state of the computation, a fixed number of equally spaced meridional half-planes is considered, including the $\varphi = 0$ half-plane and the $\varphi = \pi$ half-plane. For convenience, such number is taken as odd, so that the $\varphi = \pi/2$ half-plane belongs to the set.

In each meridional half-plane, a fixed number of equally spaced straight lines, parallel to the z axis, is considered, including the z axis itself and the $r = r_1$ line. On each $r =$ const line, a fixed number of equally spaced points is considered between the shock and the body.

Let δ be the difference between the z coordinate of a shock point and the z coordinate of a body point on a given $r =$ const line of a given $\varphi =$ const half-plane,

$$\delta = \delta(r, \varphi, t) = s(r, \varphi, t) - b(r) \tag{8}$$

and let a new set of variables, ζ, Y, X, T be related to z, r, φ, t, as follows:

$$\zeta = (z - b)/\delta \qquad Y = r \qquad X = \varphi \qquad T = t \tag{9}$$

The region to be analyzed is then mapped onto a right parallelepiped no matter what are the shapes of the body and of the shock. The z axis, which is a singular line in the cylindrical frame, is mapped onto a plane and needs a special treatment.

In the new frame, the equations of motion are

$$R_T + uR_Y + AR_X + BR_\zeta + u_Y + Eu_\zeta + (v_X + u)/Y - Fv_\zeta + w_\zeta/\delta = 0 \tag{10}$$

$$u_T + uu_Y + Au_X + Bu_\zeta - Av + G(P_Y + EP_\zeta) = 0 \tag{11}$$

$$v_T + uv_Y + Av_X + Bv_\zeta + Au + G(P_X/Y - FP_\zeta) = 0 \tag{12}$$

$$w_T + uw_Y + Aw_X + Bw_\zeta + GP_\zeta/\delta = 0 \tag{13}$$

$$S_T + uS_Y + AS_X + BS_\zeta = 0 \tag{14}$$

where

$$\left.\begin{aligned} A &= v/Y \qquad C = b'(\zeta - 1) - \zeta s_r \\ B &= [w + uC - \zeta(s_t + As_\varphi)]/\delta \\ E &= C/\delta \qquad F = \zeta s_\varphi/Y\delta \qquad G = p/\rho \end{aligned}\right\} \tag{15}$$

$$b' = db/dr \qquad \delta_r = s_r - b' \qquad \delta_\varphi = s_\varphi \qquad \delta_t = s_t \tag{16}$$

Let f be any of the parameters R, u, v, w, and S. We compute the value of f at $t = t_0 + \Delta t$ and at an interior point defined by $\zeta = \zeta_0$, $X = X_0$, $Y = Y_0$ by the formula

$$f(t_0 + \Delta t) = f(t_0) + f_T\Delta t + f_{TT}\Delta t^2/2 \tag{17}$$

where $f(t_0)$, f_T, and f_{TT} are evaluated at $t = t_0$ and at the point defined by ζ_0, X_0, Y_0. It may be noted that the underlying concept in (17) is the same as in the well-known Lax-Wendroff technique.[6] However, no equation is written here in conservation form since no sharp transitions exist between the shock and the body. The handling of the equations is consequently much simpler than the one necessary in the Lax-Wendroff technique.

The time derivatives f_T and f_{TT} can be expressed in terms of first- and second-space derivatives of f and of $s_{r\varphi}$, s_{rr}, $s_{\varphi\varphi}$, $s_{t\varphi}$, s_{tr}, s_{tt}. Their expressions are easily obtained by differentiating Eqs. (10–16), with respect to X, Y, ζ, and T. The space derivatives are computed by finite-centered differences. The values of s_t are found as explained in the following section. Then $s_{t\varphi}$ and s_{tr} are computed by finite differences. Finally, s_{tt} is computed as

$$s_{tt}(r, \varphi, t) = [s_t(r, \varphi, t) - s_t(r, \varphi, t - \Delta t)]/\Delta t \tag{18}$$

At all points on the $\varphi = 0$ and $\varphi = \pi$ half-planes, except on the z axis, suitable symmetry conditions are used. All functions except v are even in φ and X; v is odd and vanishes at all points of the symmetry plane ($\varphi = 0$, $\varphi = \pi$).

The z axis belongs to all the meridional half-planes but obviously is to be computed only once. Note (Fig. 2) that if U is the value of u in the $\varphi = 0$ half-plane, $u_\varphi = -U \sin\varphi$, $v_\varphi = -U \cos\varphi$, $v_\varphi = w_\varphi = R_\varphi = P_\varphi = S_\varphi = 0$ on the z axis. Consequently, Eqs. (10–15) become

$$R_T + uR_Y + BR_\zeta + 2u_Y + 2Eu_\zeta + w_\zeta/\delta + H = 0 \quad (19)$$

$$u_T + uu_Y + Bu_\zeta + G(P_Y + EP_\zeta) = 0 \quad (20)$$

$$v_T = 0 \quad (21)$$

$$w_T + uw_Y + Bw_\zeta + GP_\zeta/\delta = 0 \quad (22)$$

$$S_T + uS_Y + BS_\zeta = 0 \quad (23)$$

$$b' = 0 \qquad C = -\zeta s_r \qquad B = \frac{w + uC - \zeta s_t}{\delta}$$

$$A = 0 \quad (24)$$

where $H = v_{\varphi r} = v_{XY} + Ev_{X\zeta}$. In order to apply Eq. (17), Eqs. (19–24) are again differentiated with respect to Y, ζ, and T. Note that $C_Y = b''(\zeta - 1) - \zeta s_{rr}$. For convenience, H_Y and H_ζ are computed by centered finite differences, and

$$H_T(0, 0, t) = [H(0, 0, t) - H(0, 0, t - \Delta t)]/\Delta t$$

IV. Shock Points

The components of the freestream velocity in the **i**, **j**, **k** frame at a point Q on the shock are

$$u_\infty = q_\infty \sin\alpha \cos\varphi \qquad v_\infty = -q_\infty \sin\alpha \sin\varphi$$

$$w_\infty = q_\infty \cos\alpha \quad (25)$$

Since the shock is a moving surface, we define the velocity of each shock point Q in a simple way by saying that Q moves in a direction parallel to the z axis. The velocity vector **W** of a point **Q** is then obviously

$$\mathbf{W} = W\mathbf{k} = s_t\mathbf{k} \quad (26)$$

The components of the unit vector **N** normal to the shock are $-s_r/\nu$, $-s_\varphi/r\nu$, $1/\nu$, where $\nu = (1 + s_r^2 + s_\varphi^2/r^2)^{1/2}$. The normal component of the freestream velocity relative to the shock may now be computed as

$$V_{n_\infty}^{\text{rel}} = (\mathbf{V}_\infty - \mathbf{W}) \cdot \mathbf{N} \quad (27)$$

and the Rankine-Hugoniot equations are applied to find the normal component of the velocity behind the shock. The tangential component is easily evaluated and remains unchanged through the shock.

From the aforementioned considerations, we obtain one equation less than the number of unknowns (since W is unknown). The additional information is to be obtained from the inside of the shock layer. Consider an auxiliary Cartesian frame (ξ, η, ω) issuing from a point Q of the shock at the time $t = t_0 + \Delta t$. Let its ξ axis be directed along **N**. Let $\tilde{u}, \tilde{v}, \tilde{w}$ be the velocity components in the (ξ, η, ω) frame. In the (ξ, t) plane, consider the "characteristic" issuing from Q at $t = t_0 + \Delta t$ and defined by

$$d\xi/dt = \tilde{u} - a \quad (28)$$

where a is the speed of sound. The compatibility equation along such a characteristic reads

$$\frac{d\tilde{u}}{dt} - \frac{a}{\gamma}\frac{dP}{dt} = -(\tilde{v}\tilde{u}_\eta + \tilde{w}\tilde{u}_\omega) + a\left(\frac{\tilde{v}P_\eta + \tilde{w}P_\omega}{\gamma} + \tilde{v}_\eta + \tilde{w}_\omega\right) \quad (29)$$

[For more detailed information on the physical arguments

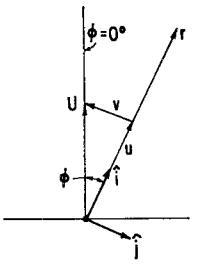

Fig. 2 Centerline velocities.

that justify the reduction of a four-dimensional problem to a single characteristic line (28) with the compatibility equation in the form (29), see Ref. 4.]

Equation (29) can now be used in addition to the Rankine-Hugoniot equations to define the shock problem fully. The equation is written in finite difference form between point Q and an initial point A^*, which is the intersection of the ξ axis ($t = t_0$) with the characteristic (28). There is no difficulty in determining A^* from (28). Once A^* is found, the values of u, v, w, P, and R are interpolated at A^* and the values of $\tilde{u}, \tilde{v}, \tilde{w}, \tilde{u}_\eta, \tilde{u}_\omega, \tilde{v}_\eta, \tilde{w}_\omega, P_\eta$, and P_ω are computed. We choose the η and ω axes as defined by two unit vectors, $\boldsymbol{\tau}$ and **b**:

$$\boldsymbol{\tau} = \text{vers}\,(\mathbf{N} \times \mathbf{j}) \qquad \mathbf{b} = \mathbf{N} \times \boldsymbol{\tau} \quad (30)$$

so that the components of $\boldsymbol{\tau}$ in the (**i**, **j**, **k**) frame are $-1/\nu_1, 0, -s_r/\nu_1$ and the components of **b** are as $s_r s_\varphi/r\nu\nu_1, -(1 + s_r^2)/\nu\nu_1, -s_\varphi/r\nu\nu_1$, where $\nu_1 = (1 + s_r^2)^{1/2}$. The relations between the (ξ, η, ω) coordinates of any point A, its cylindrical coordinates (r_A, φ_A, z_A), and the cylindrical coordinates $(r, \varphi, z = s)$ of Q are

$$-\xi s_r/\nu - \eta/\nu_1 + \omega s_r s_\varphi/r\nu\nu_1 = r_A \cos(\varphi_A - \varphi) - r$$

$$-\xi s_\varphi/r\nu - \omega(1 + s_r^2)/\nu\nu_1 = r_A \sin(\varphi_A - \varphi) \quad (31)$$

$$\xi/\nu - \eta s_r/\nu_1 - \omega s_\varphi/r\nu\nu_1 = z_A - s$$

From these equations, r_A, φ_A, and z_A can be obtained explicitly. Then their derivatives with respect to η and ω are evaluated formally. The derivative of a function f with respect to η is

$$f_\eta = f_r r_\eta + f_\varphi \varphi_\eta + f_z z_\eta \quad (32)$$

and the derivative f_ω is obtained in a similar way. Once the formal expressions for all these derivatives are obtained, they are specialized for A^* by letting $\eta = \omega = 0$. The procedure is obviously straightforward but, if written in detail, fills several pages with elementary and repetitive formulas which we consider unworthy to report here.

The whole computation of a shock point is set up in a trial-and-error form. First, a value of W at the shock point is guessed, the Rankine-Hugoniot conditions are applied, and values of P and of the normal component of the velocity behind the shock $\tilde{u}$ are obtained. Then, using this value of P, another value of $\tilde{u}$ behind the shock is computed from Eq. (29). The two values of $\tilde{u}$ are compared, and the procedure is iterated until they coincide. The value of W furnishes now the quantity s_t needed in Sec. III, and the r coordinate of the shock point can be incremented by an amount $W\Delta t$. For the shock point on the z axis, some simplifications can be made.

V. Body Points

The body points are computed in much the same way as the shock points. The components of the unit vector **N** normal to the body are $-b'/\nu, 0, 1/\nu$, where $\nu = (1 + b'^2)^{1/2}$. The velocity component normal to the body is zero at a body point Q. The pertinent information from inside the shock layer is obtained along a characteristic ending at Q at time $t = t_0 + \Delta t$ and contained in a plane defined by **N** and the time axis. Such a line comes from a point A^* located in the interior of the shock layer along **N** at $t = t_0$. Once A^* is known, the initial

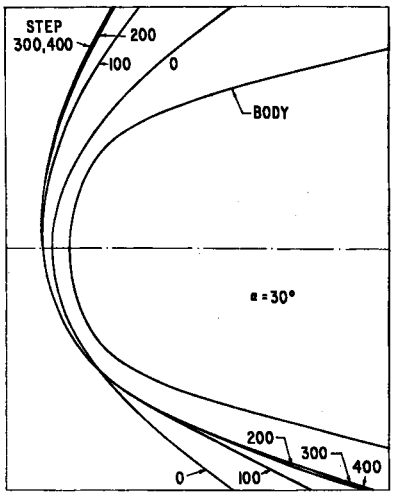

Fig. 3 Shock shape in symmetry plane as a function of time.

conditions at A^* can be determined from the neighboring points by interpolation. A Cartesian frame (ξ, η, ω) issuing from Q is considered, with Eq. (30) still holding. The characteristic to be used is defined by

$$d\xi/dt = \tilde{u} + a \tag{33}$$

The compatibility equation along its reads

$$\frac{d\tilde{u}}{dt} + \frac{a}{\gamma}\frac{dP}{dt} = -(\tilde{v}\tilde{u}_\eta + \tilde{w}\tilde{u}_\omega) - a\left(\frac{\tilde{v}P_\eta + \tilde{w}P_\omega}{\gamma} + \tilde{v}_\eta + \tilde{w}_\omega\right) \tag{34}$$

This equation is written in finite-difference form between point Q and an initial point A^*, which is the intersection of the ξ axis with the characteristic (33). The values of u, v, w, P, and R are interpolated at A^*, and the values of $\tilde{u}$, $\tilde{v}$, $\tilde{w}$, $\tilde{u}_\eta$, $\tilde{v}_\eta$, $\tilde{u}_\omega$, $\tilde{w}_\omega$, P_η, and P_ω are computed. Note that now the components of τ in the (i, j, k) frame are $-1/\nu$, 0, $-b'/\nu$ and $\mathbf{b} = -\mathbf{j}$. The relations between the (ξ, η, ω) coordinates of any point A, its cylindrical coordinates (r_A, φ_A, z_A), and the cylindrical coordinates $(r, \varphi, z = b)$ of Q are

$$-\xi b'/\nu - \eta/\nu = r_A\cos(\varphi_A - \varphi) - r$$
$$-\omega = r_A\sin(\varphi_A - \varphi) \qquad \xi/\nu - \eta b'/\nu = z_A - b \tag{35}$$

From these equations, r_A, φ_A, and z_A can be obtained explicitly. Then their derivatives with respect to η and ω are evaluated formally, and Eq. (32) is used. Finally, the formulas are specialized for A^* by letting $\eta = \omega = 0$. Note that here $\varphi^* = \varphi$ always, which makes this computation much simpler than its counterpart on the shock.

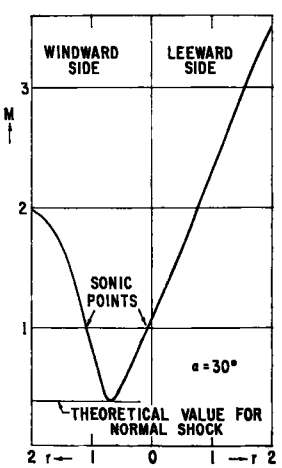

Fig. 4 Mach number distribution on intersection of shock and symmetry plane.

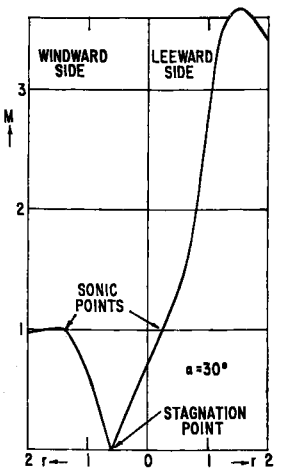

Fig. 5 Mach number distribution on intersection of body and symmetry plane.

Once the pressure at Q is found through Eq. (34) as described, the particle passing through Q at $t = t_0 + \Delta t$ is traced back to its location at $t = t_0$; and the value of S is kept constant for it since $DS/DT = 0$ [Eq. (14)]. Consequently, R is evaluated at Q. Two components of the velocity must still be computed. To this effect, two equations of motion, in the Cartesian frame (ξ, η, ω) are used:

$$\tilde{v}_t + \tilde{v}\tilde{v}_\eta + \tilde{w}\tilde{v}_\omega + (p/\rho)P_\eta = 0 \tag{36}$$

$$\tilde{w}_t + \tilde{v}\tilde{w}_\eta + \tilde{w}\tilde{w}_\omega + (p/\rho)P_\omega = 0 \tag{37}$$

In these equations $\tilde{u}$ does not appear since $\tilde{u} = 0$ on the body. Obvious simplifications are used for the body point on the z axis.

VI. Points on the Outer Boundary

The values at points located on the outer boundary ($r = r_1$) are simply extrapolated from the inner points. The errors in such values do not feed back into the computed region since the velocity at all those points is supersonic and pointing outwards.

VII. Results and Discussion

To test the program, a first computation was made for a sphere-cone at $\alpha = 0$ and $M_\infty = 4$, using three meridional half-planes only.

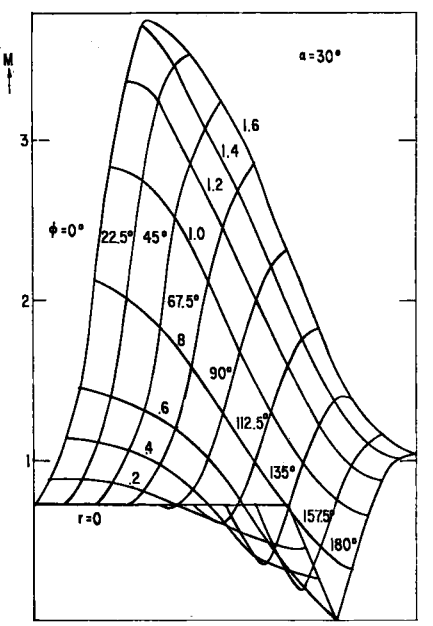

Fig. 6 Mach number distribution on the body.

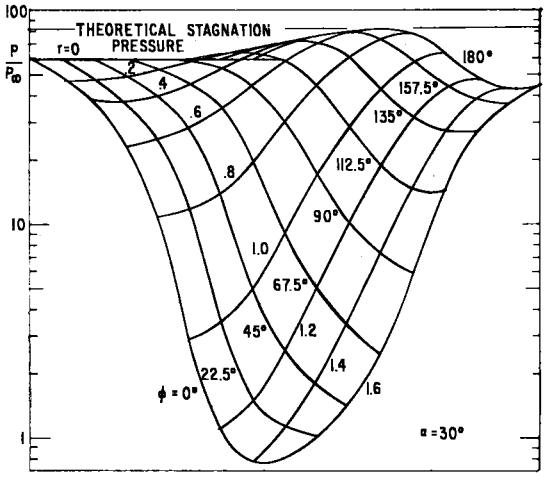

Fig. 7 Body pressure distribution.

Since this is obviously an axisymmetric problem, the results in all half-planes should be the same and equal to the results of Ref. 4. Having proved this point, a second computation was made for the same body at $\alpha = 10°$. The computation now uses the three-dimensional equations in full. The results in the subsonic-transonic region, however, should be still axially symmetric with respect to the axis parallel to $\mathbf{V}_\infty$ and issuing from the center of the sphere since the sonic line is still on the spherical portion of the body. The numerical results confirmed the theoretical predictions.

At this stage, some computations were made for bodies which generate a three-dimensional flowfield when flying at an angle of attack. Some significant results are presented here for an ellipsoid-cone (the axis of the generating ellipse is in the ratio of 1.5 to 1, and the semi-angle of the cone is 14°) at $\alpha = 30°$ and $M_\infty = 8$.

The following figures are self-explanatory. From Fig. 3 one can see how the shock (whose initial shape was purposely taken as symmetric with respect to the body axis) is changed in time until it reaches a highly unsymmetrical shape. In Fig. 4 a perfect agreement of the Mach number behind a normal shock with the computed value is found. From Fig. 5 the stagnation point can be easily detected. Figure 6 shows the Mach number distribution on the body. Figure 7 shows a similar distribution of pressures on the body. Note the perfect matching of the computed stagnation pressure with the theoretical value. The outputs, of course, provide full information at all the computed points within the shock layer so that M = const surfaces, isopycnic surfaces, isobaric surfaces, etc. can be drawn. In Fig. 8 the final section of the shock with the symmetry plane, the location of the stagnation point, and the sonic lines in the symmetry plane are shown. Figure 9 shows the steady-state shock shapes in all the meridional half-planes which were computed. Finally, Fig.

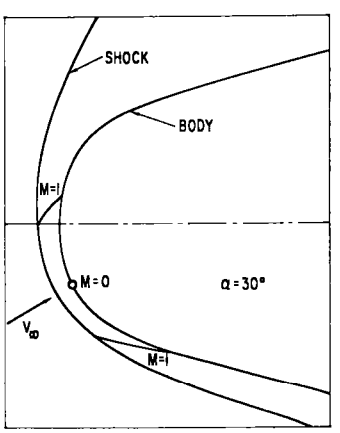

Fig. 8 Shock, sonic lines, and stagnation point in symmetry plane.

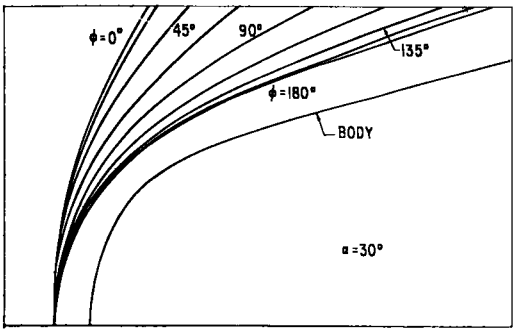

Fig. 9 Shock shape as a function of φ.

10 shows how the stagnation pressure and the standoff distance change in time (for the same ellipsoid but in the two cases of $\alpha = 20°$ and $\alpha = 30°$) and how they reach their asymptotic (steady) values. More results and a detailed description of the method can be found in Ref. 7.

In all these runs, 6 points in the z direction, 11 r = const lines on each meridional half-plane, and 9 meridional half-planes were used for a total of 594 points to be computed. Using more points was forbidden by the storage capacity of the IBM 7094 computer. However, the details of the flowfield are showing very well with such a mesh, as can be seen from the figures. With the present mesh, 300 time steps were computed in about 40 min on the IBM 7094 and in about 6 min on the CDC 6600.

The drastic reduction in running time with respect to Ref. 2 is obviously because of a comparable reduction in the number of mesh points. We observe that there is practically no difference in the number of points along the body used in Ref. 2 and in the present paper. The strongest reduction is obtained in directions pointing outward from the body (6 points instead of 48). This is a simple consequence of having assumed the shock as a discontinuity (since no point in the free-stream has to be considered). If the shock is obtained as a strong but smooth transition, a great number of otherwise nonsignificant points must be computed in front of it to permit numerical disturbances to be damped away into the free-stream (in Ref. 2, only 12 points of the 48 mentioned previously are of interest). In addition, in a purely inviscid flow a shock is a discontinuity, and treating it as a smooth transition not only affects the accuracy of the shock computation but the accuracy of the other points as well.

A similar conclusion may be reached for the body points. The characteristic technique described in the foregoing is not only very accurate but is independent of the main frame of reference. In this sense we stated in the introduction that the shape of the body may be assigned arbitrarily. Other

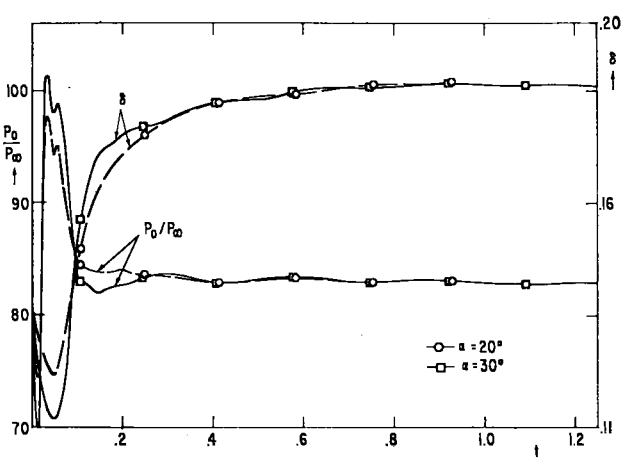

Fig. 10 Stagnation pressure and standoff distance.

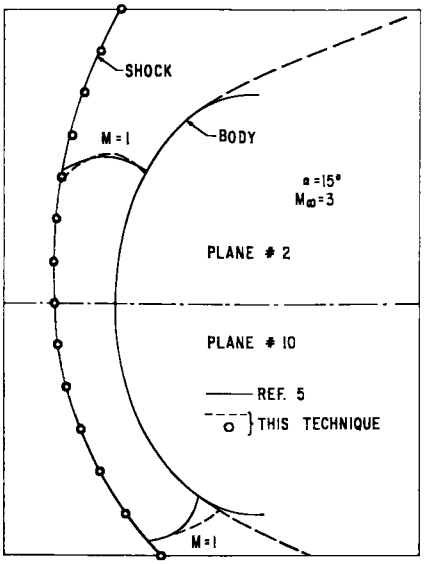

Fig. 11 Comparison of results between present technique and Ref. 5.

methods, including the one of Ref. 2, are severely limited by difficulties arising if the body is not a coordinate surface of the system of reference.

In a machine with a large core, such as the CDC 6600, a finer mesh with a greater number of points could be used. However, the running time may again reach impractical values. If all mesh sizes were reduced by a factor of 2, the running time would be multiplied by 16. We consider the mesh presently used to be a good one for all practical purposes, except if the body is extremely blunted. In all other cases, we may state that the numerical accuracy would be improved only in significant figures which are practically immaterial. The statement is supported by our experience in similar problems in two dimensions. For example, in the latter case, only the fourth significant figures are altered when a 14×21 mesh is used instead of a 7×11 mesh.

In conclusion, in Fig. 11 a comparison of some of our results with those of Ref. 5 is presented. The latter, unfortunately, was brought to our attention only when our main work was finished. Therefore, we must confine ourselves to a brief discussion. The technique used in Ref. 5 is not a time-dependent one. Using a spherical frame of reference (r, θ, φ) and a stretching of coordinates similar to the one defined by the first of Eqs. (9), the physical parameters are expressed by polynomials in θ and trigonometric polynomials in φ. The partial differential equations become ordinary differential equations in r. The technique used to solve them is not given in detail in Ref. 5. Figure 11 shows a very good agreement between our results and the results of Ref. 5.

References

[1] Swigart, R., "A theory of asymmetric hypersonic blunt-body flows," AIAA J. **1**, 1034–1042 (1963).

[2] Bohachevsky, I. O. and Mates, R. S., "A direct method for calculation of the flow about an axisymmetric blunt body at angle of attack," AIAA J. **4**, 776–782 (1966).

[3] Moretti, G. and Abbett, M., "A time dependent computational method for blunt body flows," AIAA J. **4**, 2136–2141 (1966).

[4] Moretti, G. and Abbett, M., "A fast, direct, and accurate technique for the blunt body problem," General Applied Science Labs. Inc., TR 583 (January 1966).

[5] Telenin, G. F. and Tinyakov, G. P., "A method of calculating the three-dimensional flow past a body with an attached shock wave," Soviet Phys. Doklady (English Transl.) **9**, 132–133 (1964).

[6] Lax, P. and Wendroff, B., "Difference schemes for hyperbolic equations with high order of accuracy," Comm. Pure Appl. Math. **XVII**, 381–398 (1964).

[7] Moretti, G. and Bleich, G., "A numerical technique for the three-dimensional blunt body problem," General Applied Science Labs. Inc., TR 637 (December 1966).